

# Barrier Island Elevations Relevant to Potential Storm Impacts: 1. Techniques

Nicole A. Elko, Asbury H. Sallenger, Jr., Kristy Guy, Hilary F. Stockdon, and Karen L. M. Morgan

## Introduction

A recently developed storm impact scale considers the elevation of wave runup relative to the elevation of two geomorphic parameters on barrier islands: 1) a threshold elevation, either the elevation of the foredune ridge or, if no dune is present, the elevation of the beach berm, (denoted by  $D_{high}$ ) and 2) the elevation of the base of the dune, the transition between water-laid sand of the beach and eolian deposits of the dune (denoted by  $D_{low}$ ) (Sallenger, 2000) (Figure 1). In the absence of a foredune ridge,  $D_{high} = D_{low}$  are equivalent. When compared to runup,  $D_{high}$  and  $D_{low}$  describe the nature and relative magnitude of coastal change that can be expected to occur during severe storms (Sallenger et al., 2000). For example, barrier islands with low elevations are potentially more susceptible to overwash and inundation than higher areas.

The longshore variability in  $D_{high}$  and  $D_{low}$  can be determined with high spatial resolution by utilizing a GIS-based analysis program to analyze high-density topographic data acquired with airborne scanning laser

altimetry. The key parameters,  $D_{high}$  and  $D_{low}$ , can be determined relatively quickly and efficiently by digitization in map view.

Altimetric data of the U.S. coastlines are acquired through a cooperative program between NASA and the USGS to investigate coastal change. NASA's Airborne Topographic Mapper (ATM) was developed for surveying the Greenland ice sheet (Krabill, 1995) and has been used to measure beach topography and assess coastal change in recent years (Krabill, 2000; Sallenger et al., in press a). The ATM, which is mounted on a twin-engine plane supplied by the NOAA Aircraft Operations Center, emits pulses of light and calculates the elevation of the land surface based on return time to the aircraft. These laser range data are combined with aircraft position, determined using differential global positioning system techniques, to calculate the spatial location of each point. See Brock and Sallenger (2001) for a more detailed description of laser mapping systems.

The ATM surveys a swath roughly 350-m wide, about half the nominal

survey altitude of the aircraft. The plane typically makes at least four passes of an area, producing overlapping swaths with a combined width of at least 600 m. With the capability of surveying hundreds of kilometers of coast per day, a low root-mean-squared (rms) vertical error of about 15 cm for individual laser shots (Sallenger et al., in press b), and a point density of about one point every 2 m<sup>2</sup>, the ATM provides high-quality coastal topographic surveys.

## ATM Data Conversions

To prepare ATM data for analysis, a number of processing steps are necessary to merge, sort, and convert the data to appropriate horizontal and vertical datums. The first step requires trimming three variables, longitude (x), latitude (y), and elevation (z), from the original 15-variable data files. All of the swaths recorded on the same day are then merged into one file. ATM data are acquired in ITRF97 (IERS (International Earth Rotation Service) Terrestrial Rotation Frame 1997) relative to the WGS84 ellipsoid and are converted to

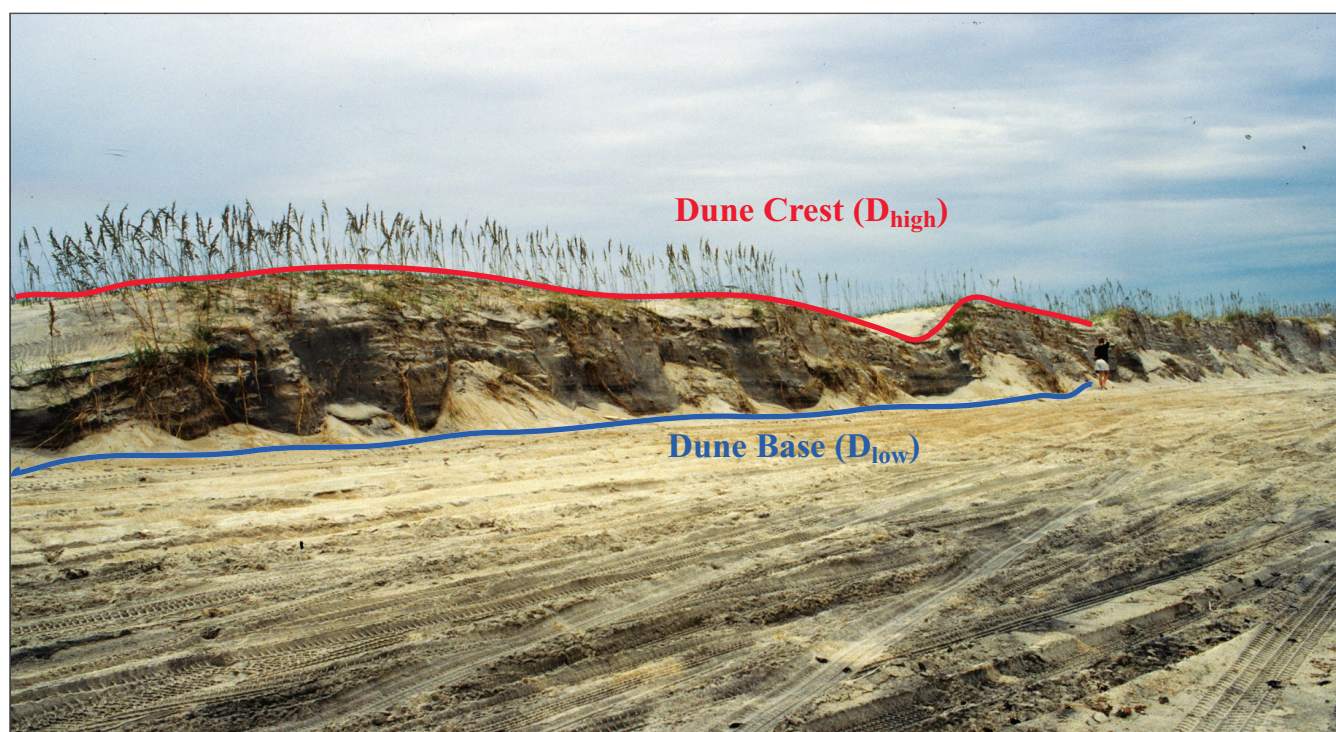


Figure 1. Illustration of geomorphic features important in assessing vulnerability and determining coastal change. The location of the dune crest ( $D_{high}$ ) and the dune base ( $D_{low}$ ) are drawn on a photograph of dunes north of Rodanthe, North Carolina.

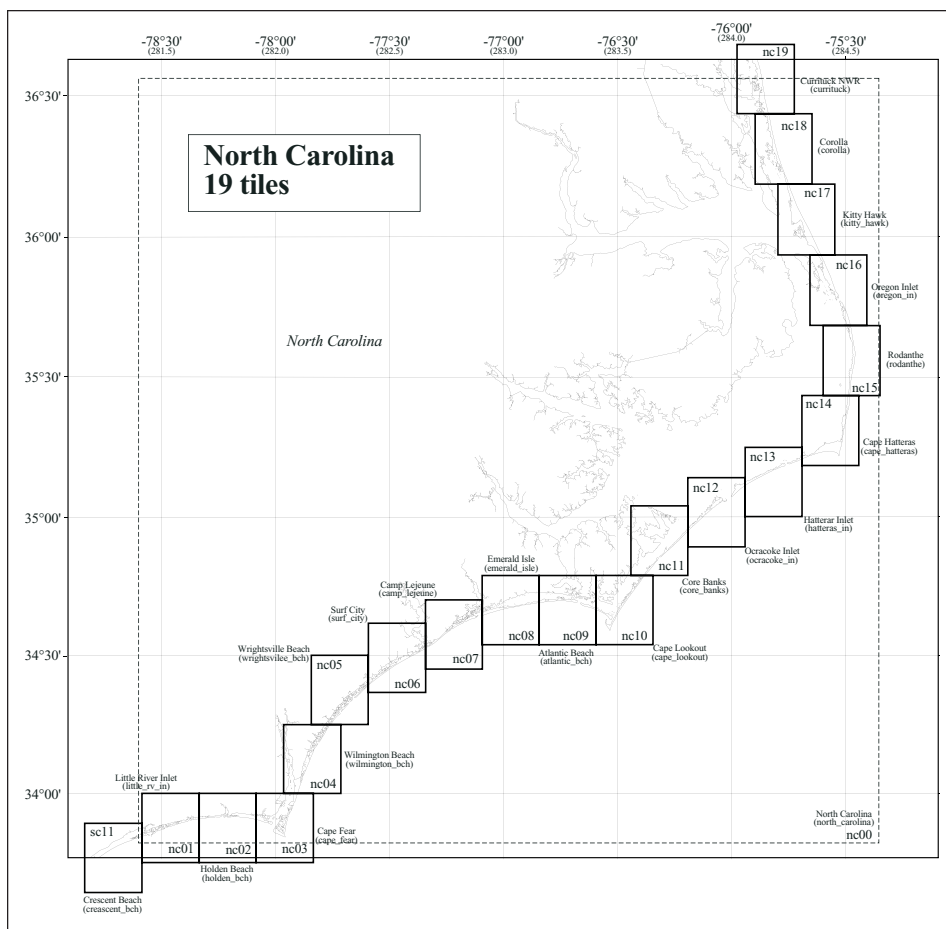


Figure 2. Example of tile-sized ( $0.25^\circ$ ) squares of lidar data that are merged and converted from raw altimetry data and saved as ASCII files, then TINned and gridded to create DEMs.

NAD83 and NAVD88 horizontal and vertical datums respectively. The new coordinates for each flight are sorted by latitude or longitude depending on shoreline orientation. Then, the data are divided into manageable-sized tiles measuring  $0.25^\circ$  per side (Figure 2) and saved as ASCII files. Merging, sorting, and converting the data from one flight (comprising 200 to 300 km of coast) in the ITRF97/WGS84 format takes about 48 hours on a Sun UltraSPARC-II 400MHz processor.

The ASCII files, which usually contain about five million randomly scattered points each, are divided into one million point files and used to create a triangulated irregular network (TIN) surface model. The TINning process uses the Delaunay method of triangulation wherever possible, connecting each sample point to its two nearest neighbors. A digital elevation model (DEM) is interpreted from the TIN by creating a lattice of sampling points spaced 1-m apart in both the x and y directions and linearly interpolating the z-values from the TIN.

To prepare the data for digitizing, the elevation grids are merged to form two or three 100-MB images of continuous raster

data for each tile. TINning, gridding, and creating images for one tile of data (comprising about 25 km of coast) takes approximately three hours on a 667 MHz, Pentium III processor.

## Data Analysis

Once the elevation images are produced, a team of computer operators performs a semi-automated two-part analysis: 1) digitizing the approximate locations of the threshold elevation ( $D_{high}$ ) and the dune base ( $D_{low}$ ); and 2) utilizing a GIS-based program that automatically seeks the actual height of  $D_{high}$  and  $D_{low}$  values within a buffer around the digitized line. Due to the unpredictable form and location of coastal topography, and anthropogenic alteration of many coasts, a fully automated algorithm for finding  $D_{high}$  and  $D_{low}$  is not feasible at this stage.

## Digitization

Gray-scale images of slope, aspect, and the slope of the slope (second derivative of elevation) are created from elevation images (Figures 3 and 4). Blue colors in the elevation images correspond to water, dark gray colors correspond to relatively low

elevations (beach, roads, parking lots), and light gray colors correspond to relatively high elevations (dunes, houses). The elevation image has two primary functions: 1) as a reference image (Figures 3 and 4) alongside the slope and aspect images during digitization, and 2) as input to the models that calculate the exact location and elevation of  $D_{high}$  and  $D_{low}$ .

## $D_{high}$

In the example aspect image (Figure 3B), dark gray colors represent land or water surfaces that slope seaward and light gray colors represent surfaces that slope landward. The contact between dark and light gray (i.e. between seaward-sloping and landward-sloping regions) highlights the location of the dune crest, or berm crest if no dunes are present. Operators digitize along this contact to determine the first approximation of the location of  $D_{high}$ .

Computer operators digitize the approximate location of  $D_{high}$  by viewing both the elevation and aspect images side-by-side and “geo-linking” the images, so that both viewers show the same spatial coverage of an area and scroll up/down simultaneously (Figure 3). The elevation image serves as a snapshot of the area and the line (shown in red) which delineates the location of  $D_{high}$  is digitized on the aspect image. A cross-shore profile with a linked crosshair aids the operators in their placement of the digitized line (Figure 3C).

## $D_{low}$

In the example slope image (Figure 4B), dark gray colors correspond to relatively flat slopes and light gray colors correspond to relatively steep slopes. The contact between dark and light gray (i.e. between the flat beach and the steep dune face) delineates the location of the dune base. This line (shown in blue) is digitized as the first approximation of the location of  $D_{low}$ .

The same procedure is followed for approximating  $D_{low}$  with the exception that the line is digitized on the slope image (Figure 4).  $D_{low}$  is generally the more difficult parameter to determine because its definition is more subjective than that of  $D_{high}$  (e.g. consider a gently sloping dune with no distinct break between dune face and beach).

## Computer Model

After digitizing the approximate locations of  $D_{high}$  and  $D_{low}$ , operators execute a GUI-driven model to refine the spatial location of the parameters. The model uses the digitized line as a guide and

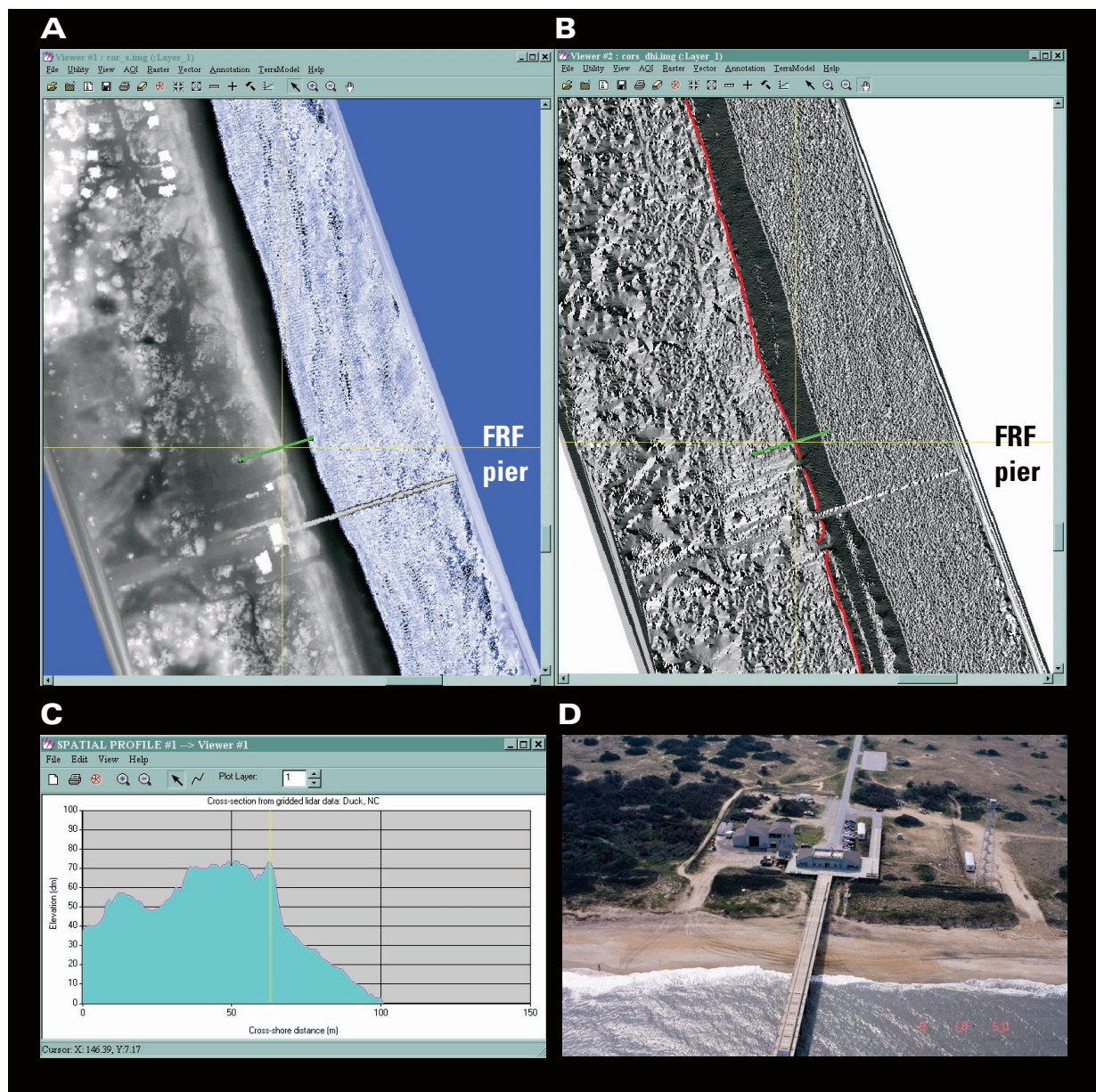


Figure 3. Digitization of the threshold elevation at the U.S. Army Corps of Engineers Field Research Facility (FRF) in Duck, NC, A) grayscale elevation image, B) aspect image: dark grays = seaward slopes and light grays = landward slopes, C) cross-shore profile shown in green is linked to elevation and aspect images by yellow cross-hair on  $D_{high}$ . The digitized approximation of  $D_{high}$  appears as a red line on the aspect image. D) Aerial photo of the FRF.

creates a new raster image of the elevation and location of  $D_{high}$  and  $D_{low}$ .

To determine the threshold elevation, a 7-m wide analysis area is created around the digitized line. Then a neighborhood function, operating on a row-by-row basis, selects the maximum elevation value within the buffer. Essentially, the model treats each row, column, or diagonal, depending on shoreline orientation, of the 1-m grid as a cross-shore profile and searches for the maximum elevation in the vicinity of the digitized line. The result is a single  $D_{high}$  value for every meter alongshore.

The algorithm for determining the dune base is similar, but with two differences: the

analysis area around the digitized line is only 3-m wide, and the neighborhood function selects as the dune base pixel with the maximum value of the second derivative of elevation. In other words, the location with the most rapidly changing slope (steepest location) in the vicinity of the digitized line is selected as the base of the dune. A smaller buffer is necessary in this case to avoid selecting small perturbations with rapidly changing slopes near the dune base.

Once the images of  $D_{high}$  and  $D_{low}$  are produced, operators must quality-check the images. Any unnatural features such as houses, walkovers, or anomalous points that were captured by the model must

be removed from the image. Lastly, the images go through a final quality-check performed by the project leader who checks, for example, that pixels selected as  $D_{high}$  represent the highest elevation on the first foredune ridge and pixels selected as  $D_{low}$  represent the dune base, not a small perturbation in the vicinity of the dune base. Additionally, the project leader checks that the  $D_{high}$  pixels represent an objective, continuous dune or berm line without spikes that extend to a higher dune ridge landward of the first foredune ridge.

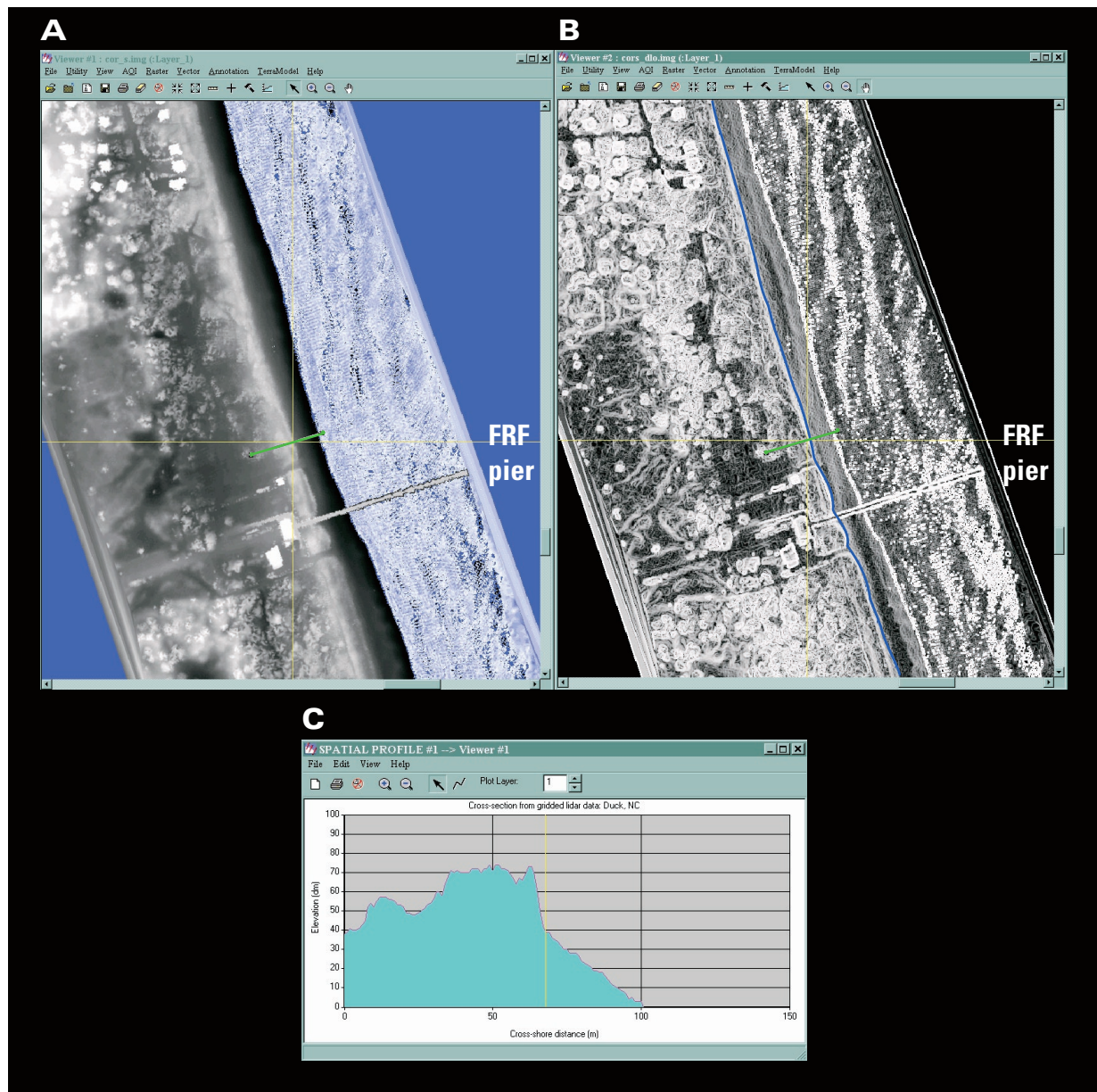


Figure 4. Digitization of the dune base at the U.S. Army Corps of Engineers FRF, A) grayscale elevation image, B) slope image: dark grays = relatively flat slopes (beach) and light grays = relatively steep slopes (dune face), C) cross-shore profile shown in green is linked to elevation and aspect images by yellow cross-hair (on  $D_{low}$ ). The digitized approximation of the dune base appears as a blue line on the slope image.

## Repeatability

Most procedures involving manual digitization of spatial locations introduce some degree of subjectivity. To determine the precision of the procedure used here, five different operators performed replicate digitizations of two different images. The first image is a subset of Fernandina Beach, an area on Amelia Island in northeast Florida with well-developed foredune ridges, topographically similar to the beaches along the northern Outer Banks of North Carolina (Figures 3 and 4). In both areas, houses are built on and landward of the high continuous dunes, and wooden walkovers frequently transit the dune crest. The second image is from Venice, a beach on the west

coast of Florida. There, dunes are very low or absent, and development is ubiquitous (Figure 5). In some cases, seawalls are the highest elevation on the beach, and in others, dunes are absent and the berm is the highest elevation.

Repeatability was examined by calculating differences in  $D_{high}$  and  $D_{low}$  results between a single operator (called the standard operator) and the other four operators. Note that the mean differences, for  $D_{high}$  for Fernandina Beach for example, all have the same sign, indicating that the operator chosen to compare to each of the others (the standard operator) was at one extreme of the observed offsets. If an operator that was more central in offset

had been chosen as the standard, the error estimates would have been smaller.

Elevation values for  $D_{high}$  or  $D_{low}$  determined by the standard operator ( $z_s$ ) were subtracted from elevation values determined by the other four individuals ( $z_i$ ) to arrive at an elevation difference ( $z_{si}$ ) for each of the four operators. Three statistics were calculated to describe the error of the procedure: 1) mean error,  $\mu_{si}$ , the mean difference, or offset, between a standard and an individual operator,

$$\mu_{si} = \frac{\sum_{x=1}^N z_{si}(x)}{N}$$

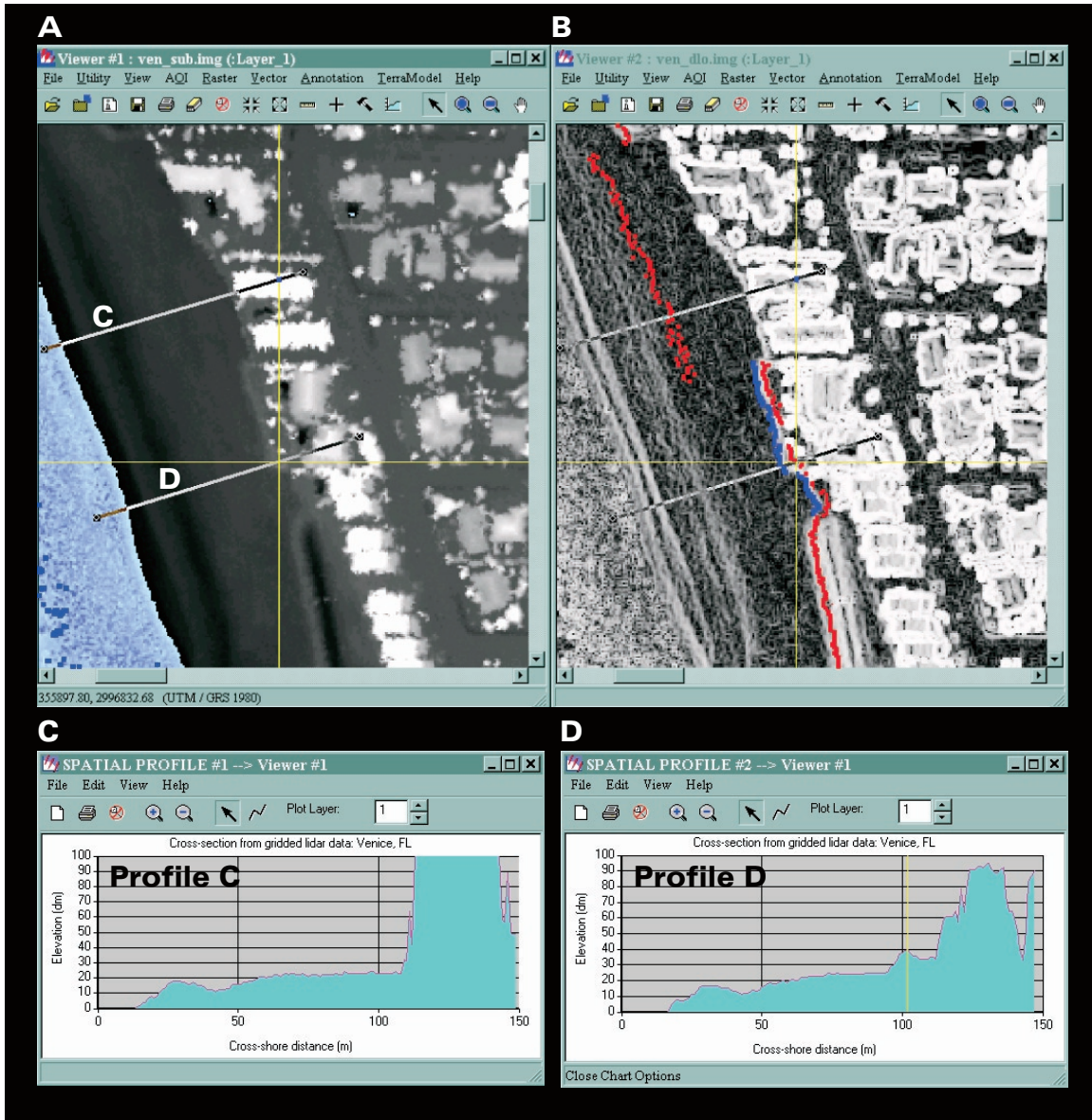


Figure 5. Digitization of  $D_{high}$  and  $D_{low}$  at Venice, located on the west coast of Florida, A) elevation and B) slope images illustrating the locations of  $D_{high}$  (red points) and  $D_{low}$  (blue points) in areas of berms, dunes, and seawalls. C) No dune is present on Profile C; therefore, the berm represents  $D_{highr}$  and no  $D_{low}$  (dune base) exists. D) The dune crest is  $D_{high}$  on Profile D, and  $D_{low}$  is defined. A seawall, which also has no dune base, occupies the southern third of images A and B.

where  $N$  is the number of  $D_{high}$  or  $D_{low}$  values in the image, 2) random error,  $\sigma_{si}$ , the standard deviation about the mean of the differences between the standard and each individual operator,

$$\sigma_{si} = \sqrt{\frac{\sum_{x=1}^N (z_{si}(x) - \mu_{si})^2}{N}}$$

and 3) total error, the rms of the differences or, the combined mean and random error between the standard operator and the individual operators ( $rms_{si}$ ),

$$rms_{si} = \sqrt{\frac{\sum_{x=1}^N z_{si}(x)^2}{N}}.$$

Low error estimates for Fernandina Beach  $D_{high}$  comparisons ( $\mu = 0.01$  m and  $rms = 0.05$  m) indicate that results there were highly repeatable between operators (Table 1). The largest rms error of 0.07 m is well within the rms error of the ATM (0.15 m). These results are generally applicable to areas with a straight, easily identifiable, and continuous foredune ridge, such as many North Carolina beaches (Figures 3 and 4). Larger rms errors for  $D_{low}$  (0.50 m) reflect the greater difficulty involved in choosing this parameter.

$D_{high}$  and  $D_{low}$  replicates for the complex environment of Venice were more scattered due to the subjectivity involved in choosing among seawalls, berms, and very low dunes (Figure 5). Rms error for  $D_{high}$  in this region was 0.69 m and rms error for  $D_{low}$  was 0.23 m (Table 1). This scenario represents the approximate worst-case.

Unlike our operational procedure, no final quality-check was performed on the images in this repeatability analysis. Typically, operators complete  $D_{high}$  and  $D_{low}$  images and transfer them to the project leader who reviews all the images and makes changes necessary to minimize variability among different operators. This is a conservative approach to error analysis due to the lack of a final quality check (see

	$\mu$ (m)	$D_{high}$ $\sigma$ (m)	rms (m)	$\mu$ (m)	$D_{low}$ $\sigma$ (m)	rms (m)
<b>Fernandina Beach, FL</b>						
A	0.01	0.06	0.06	-0.25	0.45	0.52
B	0.02	0.07	0.07	-0.35	0.42	0.53
C	0.00	0.04	0.04	-0.32	0.34	0.49
D	0.00	0.04	0.04	0.15	0.43	0.46
Average	0.01	0.05	0.05	-0.19	0.41	0.50
<b>Venice, FL</b>						
A	-0.44	0.74	0.87	-0.00	0.14	0.14
B	0.19	0.32	0.38	0.02	0.12	0.13
C	-0.33	0.67	0.75	-0.20	0.40	0.46
D	-0.30	0.67	0.74	-0.03	0.20	0.21
Average	-0.22	0.60	0.69	-0.06	0.22	0.23

Table 1. Mean ( $\mu$ ), random ( $\sigma$ ), and rms error comparison for  $D_{high}$  and  $D_{low}$  of two different beaches that were digitized by five operators. Errors were calculated by subtracting values determined by four of the operators from a standard operator.

## References

- Brock, J. and Sallenger, A.H., Jr., 2001, Airborne Topographic Lidar Mapping for coastal science and resource management, *USGS Open File Report 01-46*.
- Krabill, W.B., Wright, C.W., Swift, R.N., Fredrick, E.B., Manizade, S.S., Yungel, J.K., Martin, C.F., Sonntag, J.G., Duffy, M., Hulslander, W., and Brock, J.C., 2000, Airborne laser mapping of Assateague National Seashore beach, *Photogrammetric Engineering and Remote Sensing*, v. 66, no. 1, p. 65-71.
- Krabill, W.B., Thomas, R.H., Martin, C.F., Swift, R., and Frederick, E.B., 1995, Accuracy of airborne laser altimetry over the Greenland ice sheet, *Int. Journal of Remote Sensing*, v. 16, p. 1211-1222.
- Sallenger, A.H., Jr., 2000, Storm impact scale for barrier islands, *Journal of Coastal Research*, v. 16, no. 3, p. 890-895.
- Sallenger, A. H., Jr., Stockdon, H., Haines, J., Krabill, W., Swift, R., and Brock, J., 2000, Probabilistic assessment of beach and dune changes, *Coastal Engineering 2000*, p. 3035-3047.
- Sallenger, A.H., Jr., Krabill, W.B., Swift, R.N., Brock, J.C., List, J., Hansen, M., Holman, R.A., Manizade, S.S., Sonntag, J.G., Meredith, A., Morgan, K., Yunkel, J.K., Frederick, E.B., and Stockdon, H., in press a, Evaluation of airborne topographic lidar for quantifying beach changes, *Journal of Coastal Research*.
- Sallenger, A.H., Jr., Krabill, W.B., Brock, J.C., Swift, R.N., Manizade, S.S., Stockdon, H., and Hampton, M., in press b, Sea-cliff erosion as a function of beach changes and extreme wave runoff during the 1997-98 El Niño, *Marine Geology*.

previous section for description), and in an actual application of the procedure, errors are likely to be lower.

## Summary

A procedure for extracting two morphologic quantities,  $D_{high}$  and  $D_{low}$ , from high-resolution altimetry data has been developed. A number of processing steps merge, sort, and convert the data to the NAD83 horizontal datum and the NAVD88 vertical datum. GIS software is then used to TIN and grid the data with 1-m resolution. A team of computer operators digitizes the approximate location of  $D_{high}$  on aspect images and  $D_{low}$  on slope images, before utilizing a program that refines the spatial location and elevation of  $D_{high}$  and  $D_{low}$ . The results undergo a final quality check by the project leader who checks every image for consistency.  $D_{high}$  and  $D_{low}$  elevations for the South Atlantic and the Gulf of Mexico United States coastlines will provide two useful parameters for scientists attempting to understand the causative mechanisms of longshore variability in shorelines and dunes (e.g., erosional hot spots) and to forecast coastal change caused by severe storms.

## Acknowledgements

We thank Eric Nelson, Meg Palmsten, Lauren Shapiro and Lance Thornton for digitizing  $D_{high}$  and  $D_{low}$  for the repeatability analysis, and Peter Howd for helpful error discussions. Reviewers Tonya Clayton and John Brock also provided insightful comments.

## Contact Information:

Nicole A. Elko  
Email: [nelko@usgs.gov](mailto:nelko@usgs.gov)  
Telephone: 727-803-8747 x 3119

Asbury Sallenger  
Email: [asallenger@usgs.gov](mailto:asallenger@usgs.gov)  
Telephone: 727-803-8747 x 3015

U.S. Geological Survey  
Center for Coastal Geology  
600 4th Street South  
St. Petersburg, FL 33701

Learn more on the Web:  
<http://coastal.er.usgs.gov/hurricanes>